Available online at www.sciencedirect.com

SciVerse ScienceDirect

Ceramics International 39 (2013) 7975–7982

CERAMICS INTERNATIONAL

www.elsevier.com/locate/ceramint

Structural and electrical properties of $La_{0.7}Sr_{0.3}Co_{0.5}Fe_{0.5}O_3$ powders synthesized by solid state reaction

Rodrigo V. da Côrte, Leandro da Conceição, Mariana M.V.M. Souza*

School of Chemistry—Federal University of Rio de Janeiro (UFRJ), Centro de Tecnologia, Bloco E, sala 206, CEP 21941-909, Rio de Janeiro/RJ, Brazil

Received 17 February 2013; received in revised form 16 March 2013; accepted 18 March 2013
Available online 23 March 2013

Abstract

This work investigates the effect of synthesis parameters (calcination temperature, milling conditions and sintering temperature) on the structural, morphological and electrical properties of $La_{0.7}Sr_{0.3}Co_{0.5}Fe_{0.5}O_3$ (LSCF) powders prepared by the solid state reaction. The thermogravimetric profile showed that the minimum temperature needed for the carbonate decomposition and formation of perovskite phase is 800 °C. SEM analysis revealed the loose and porous structure of the powder materials. The XRD patterns demonstrate that milling parameters such as grinding balls:sample ratio, rotational speed, and milling time influence the structural properties. The results revealed that powders synthesized with grinding balls:sample ratio of 8:1, 500 rpm and 4 h of milling present pure LSCF phase. Porosity of the pellets decreased with increasing sintering temperature from 950 to 1100 °C. Electrical conductivity was measured at 400–1000 °C and correlated with sintering temperature.

Keywords: Sintering; Solid state; Mechanochemical synthesis; LSCF

1. Introduction

Perovskite-type oxides $LaMO_3$ (M = Mn, Co, Fe and Ni) have been widely investigated as potential oxidative catalysts and electrodes for solid oxide fuel cells (SOFC), because they are able to reduce molecular oxygen and transport oxide ions [1]. Particularly, $La_{1-x}Sr_xCo_{1-y}Fe_yO_3$ (LSCF) compositions have attracted substantial interest because of their superior mixed electronic–ionic conduction, which make them promising cathode materials for intermediate temperature solid oxide fuel cells (IT-SOFC) [2,3].

The structural and electrical properties of LSCF oxides depend greatly on their composition and synthesis method. An appropriate synthesis condition of powder is very important because this affects several properties such as phase purity and particle size. A coarse structure improves gas permeability and ionic and electronic conductivities, while a fine structure leads to a high specific surface area and therefore to a large number of reaction sites [4].

Several synthesis methods have been used for preparation of perovskite powders, such as solid state reaction, combustion method and some chemical solution methods, for example, sol–gel, coprecipitation, and citrate process [5–8]. The solid state reaction is a conventional method of ceramic processing; it is simple and low-cost to operate and uses cheap and easily available oxides as starting materials. However, this method usually involves high temperatures and leads to large particle sizes and limited degree of chemical homogeneity [9,10]. Thus, more detailed studies regarding the influence of synthesis parameters are needed to reduce the processing temperatures and improve structural properties.

Zhang et al. [9,11] synthesized $LaMnO_3$ using a high-energy ball mill at room temperature, producing fine powders with large surface area. It is known that the chemical reactivity of starting materials can be improved significantly after mechanochemical activation and, subsequently, the calcination temperature is reduced [12]. The mechanochemical method is characterized by the repeated welding, deformation and fracture of the constituent powder materials. With continued mechanical deformation there is an increase in surface energy, which may affect the structural and physico-chemical properties of the material [13]. Using the

*Corresponding author. Tel.: +55 21 25627598; fax: +55 21 25627596.
E-mail address: mmattos@eq.ufrj.br (M.M.V.M. Souza).

0272-8842/$ - see front matter © 2013 Elsevier Ltd and Techna Group S.r.l. All rights reserved.
http://dx.doi.org/10.1016/j.ceramint.2013.03.063

mechanochemical processing, it is possible to produce nanoparticles with narrow size distribution and uniformity of crystal structure and morphology [14].

Although many studies use solid state reaction for synthesizing perovskite oxides, there is a lack of a systematic study of the influence of the main synthesis parameters on the powder properties. The objective of this work is to study the effect of the calcination temperature and milling parameters (balls:sample weight ratio, rotational speed and milling time) on the structural properties of $La_{0.7}Sr_{0.3}Co_{0.5}Fe_{0.5}O_3$ (LSCF) powders synthesized by solid state reaction. The porosity and electrical conductivity of LSCF pellets were also investigated after sintering at different temperatures.

2. Experimental

2.1. Synthesis

The starting materials used in this study were metal oxides (La_2O_3, Fe_2O_3 and Co_3O_4) and strontium carbonate ($SrCO_3$). All reagents were supplied from Vetec (Brazil), with purity $>99.9\%$. The mixture of oxides and carbonate was placed in a zirconia pot of 125 mL together with zirconia balls of 10 mm diameter and milled in a planetary ball mill Retsch PM 100. The mass ratio of balls and starting materials (8:1 and 6:1), the rotational speed (300, 400, 500 and 600 rpm) and milling time (2, 4 and 6 h) were evaluated.

In order to evaluate the influence of calcination temperature on the perovskite phase formation, one sample was synthesized with balls:materials ratio of 8:1, 500 rpm and total milling time of 6 h. The powder was then calcined at 500, 600, 700, 800, 900 and 1000 °C for 10 h, with a heating rate of 10 °C min^{-1}.

The powders were uniaxially pressed with 2 t loading and the green pellets (13 mm diameter and 2 mm thickness) were sintered at 950–1100 °C for 4 h with a heating rate of 10 °C min^{-1}.

2.2. Characterization

Thermogravimetric analysis (TGA) of the as-prepared powder was carried out using a TA thermal analyzer (SDT Q600), with a heating rate of 5 °C min^{-1} from room temperature to 1000 °C in air.

The prepared powders were analyzed by X-ray diffraction (XRD), in a Rigaku Miniflex II diffractometer with monochromator, using CuKα radiation ($\lambda = 1.5405$ Å), speed of 2° min^{-1} and over the 2θ range of 10° and 90°. The crystallite sizes (D_{XRD}) and microstrain (ε) were calculated using the model proposed by Williamson and Hall [15], by means of the following formula:

$$\beta cos\,\theta/\lambda = 1/D_{XRD} + 4\varepsilon sin\,\theta/\lambda \quad (1)$$

where θ is the diffraction angle, λ is the wavelength of incident radiation and β is the full width at half maximum (FWHM) of the peak. Plotting the $\beta \cos\theta/\lambda$ versus $4 \sin\theta/\lambda$ a straight line yields the crystallite size from interception with the ordinate and microstrain from the slope.

The microstructure of LSCF powders and pellets was investigated by scanning electron microscopy (SEM) using Hitachi TM-1000 equipment. The acceleration voltage was 15 kV, using backscattering electron.

The apparent densities of the LSCF sintered pellets were determined by the Archimedes method using water and the porosity was calculated by the following equation:

$$P = [(\rho_t - \rho_A)/\rho_t]100 \quad (2)$$

where P is the porosity (%), ρ_t is the theoretical density (g cm^{-3}) and ρ_A is the apparent density (g cm^{-3}).

Electrical conductivity of the sintered pellets was measured by DC two-probe technique, with a HP 34420A multimeter, using platinum electrodes in a thermoelectric furnace MAITEC, at temperature range of 400–1000 °C. The electrical conductivity measurements were repeated twice on each pellet; the values varied less than 10% under the experimental conditions used.

3. Results and discussion

3.1. Effect of the calcination temperature

Fig. 1 shows TGA curve of the as-synthesized LSCF powder, before calcination. Thermal decomposition takes place in two stages and the weight loss is complete at about 800 °C. The first decomposition stage, up to 400 °C, can be assigned to the loss of adsorbed water and carbon dioxide, which is a common feature in mechanically activated materials [16]. The second stage, at about 550–800 °C, can be associated with complete decomposition of carbonate that remained after milling, as also observed by Moure at al. [17]. The total weight loss is about 8%, and the second stage represents 6%.

Fig. 2 shows the XRD patterns of the as-synthesized sample and samples calcined at different temperatures, from 500 to 1000 °C. The non-calcined sample presented an incipient formation of perovskite phase, with peaks attributed to $SrCO_3$ (JCPDS 5-418). This carbonate phase is still present in the

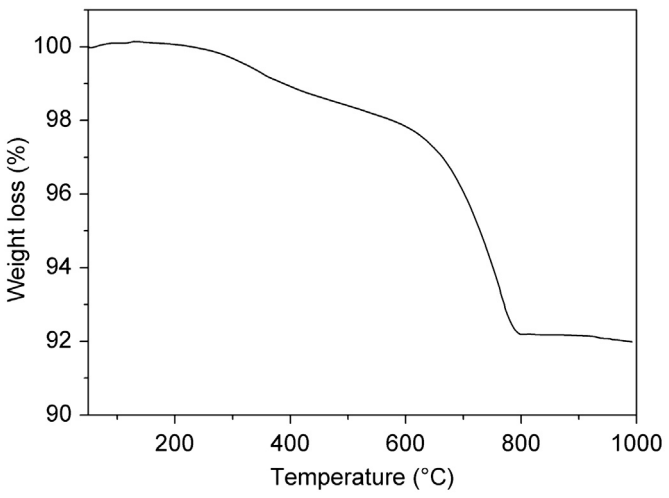

Fig. 1. TGA curve of the as-synthesized LSCF powder prepared by solid state reaction.

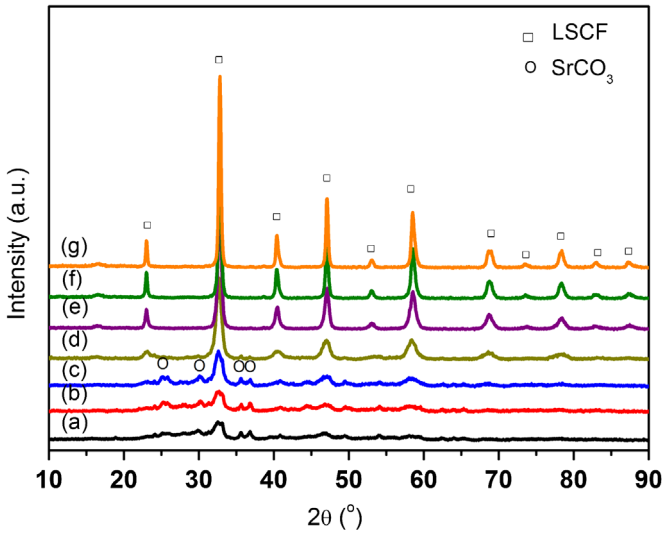

Fig. 2. XRD patterns of LSCF powders: non-calcined (a) and calcined at different temperatures: (b) 500 °C, (c) 600 °C, (d) 700 °C, (e) 800 °C, (f) 900 °C and (g) 1000 °C.

Table 1
Average crystallite size (D_{XRD}), microstrain (ε) and lattice parameters of LSCF samples calcined at different temperatures.

Calcination temperature (°C)	D_{XRD} (nm)	ε(%)	Lattice parameters (Å)
700	9.6	1.09	a = 5.4717 ± 0.0082 c = 3.3020 ± 0.0450
800	15.5	0.68	a = 5.4592 ± 0.0047 c = 13.3252 ± 0.0258
900	22.5	0.46	a = 5.4622 ± 0.0036 c = 13.3463 ± 0.0198
1000	25.9	0.40	a = 5.4659 ± 0.0034 c = 13.3300 ± 0.0186

samples calcined up to 600 °C. The perovskite phase (ICSD 512822) appears with well defined peaks after calcination at 700 °C and its peak intensity increases gradually as the calcination temperature increases to 1000 °C. The carbonate phase completely disappears after calcination at 800 °C, in agreement with TGA results. This temperature will be used for calcination of all samples prepared hereafter.

When solid state reaction is used to synthesize perovskites without previous milling, the calcination is carried out at higher temperatures and/or longer times. Wandekar et al. [18] calcined oxides of La, Mn, Co and $SrCO_3$ during 6 days at 900 °C to obtain $La_{0.76}Sr_{0.19}Mn_{1-y}Co_yO_{3\pm\delta}$. Nityanand et al. [19] obtained pure perovskite phase for LSCF samples synthesized by solid state reaction only after calcination at 950 °C for 10 days, while Möbius et al. [20] used calcination at 1150 °C for 24 h. Thus, the activation by milling is an essential step to synthesize LSCF powders with single phase at low calcination temperatures.

Table 1 shows the average crystallite size (D_{XRD}) and microstrain (ε) of the samples calcined from 700 to 1000 °C, and the lattice parameters of the perovskite structure. All samples presented rhombohedral structure (space group R3c) with lattice parameters close to those of ICSD 512822 ($a = 5.460$ and $c = 13.244$ Å). The rhombohedral symmetry was also observed by Tai et al. [21] for $La_{0.8}Sr_{0.2}Co_{1-y}Fe_yO_3$ samples with $0 \le y \le 0.7$. The crystallite size increases with increasing calcination temperature while the microstrain decreases. The crystallite sizes obtained here are very similar to those reported for LSCF samples prepared by the combustion method and calcined at 750 °C (9–20 nm) [8] or 825 °C (19–24 nm) [22]. The crystallite size of LSCF sample prepared by the solid state reaction and calcined at 950 °C for 10 days was 22 nm, according to Nityanand et al. [19].

The morphology of the particles in ceramic materials is a consequence of the preparation method and thermal treatment. Fig. 3 shows SEM analysis of LSCF powders calcined at different temperatures. The materials prepared by solid state reaction showed a spongy aspect and the particles are linked together in agglomerates of different sizes with no significant local sintering among them. The particle size slightly increases with increasing calcination temperature, while the apparent porosity decreases.

3.2. Effect of the milling parameters

The first parameter studied was the mass ratio between the balls and the sample. XRD patterns of the samples synthesized with 500 rpm, 6 h of milling and different balls:sample ratios are shown in Fig. 4A. The sample synthesized with 8:1 ratio presented a single perovskite phase, while secondary phases of $SrCO_3$ and La_2O_3 (JCPDS 5-602) are also observed when 6:1 ratio was used. Attempting to decrease the formation of these secondary phases, the milling time for the sample prepared with 6:1 ratio was increased to 8 and 10 h, and XRD patterns are shown in Fig. 4B. The increase in the milling time up to 10 h was not enough to provide single phase formation, showing that an adequate amount of balls is essential in mechanochemical activation.

The second parameter investigated was the rotational speed, which was varied from 300 to 600 rpm, for the sample prepared with balls:sample ratio of 8:1 and 6 h of milling. XRD patterns (Fig. 5A) show the formation of the perovskite phase for all samples, but that synthesized at 300 rpm also presented secondary phases of La_2O_3 and Co_3O_4 (JCPDS 42-1467), indicating that oxide precursors are still present when this low speed is used. The crystallite sizes of the perovskite phase are 12–15 nm, with lower microstrain (0.68%) for the sample synthesized at 500 rpm, indicating a crystalline lattice with lower internal stress.

Finally, the effect of milling time was investigated, using balls:sample ratio of 8:1 and 500 rpm, on the phase formation of LSCF powders (Fig. 5B). The samples synthesized with 4 and 6 h of milling presented single perovskite phase formation, while it is possible to observe a very small contribution of $SrCO_3$ for the sample milled for only 2 h. Thus, a minimum of 4 h milling is desirable for complete formation of the perovskite phase. Table 2 shows the crystallite size and microstrain of the samples synthesized with different milling times, and the lattice parameters of the perovskite structure. There is a slight increase in the crystallite size with milling time, while microstrain decreases.

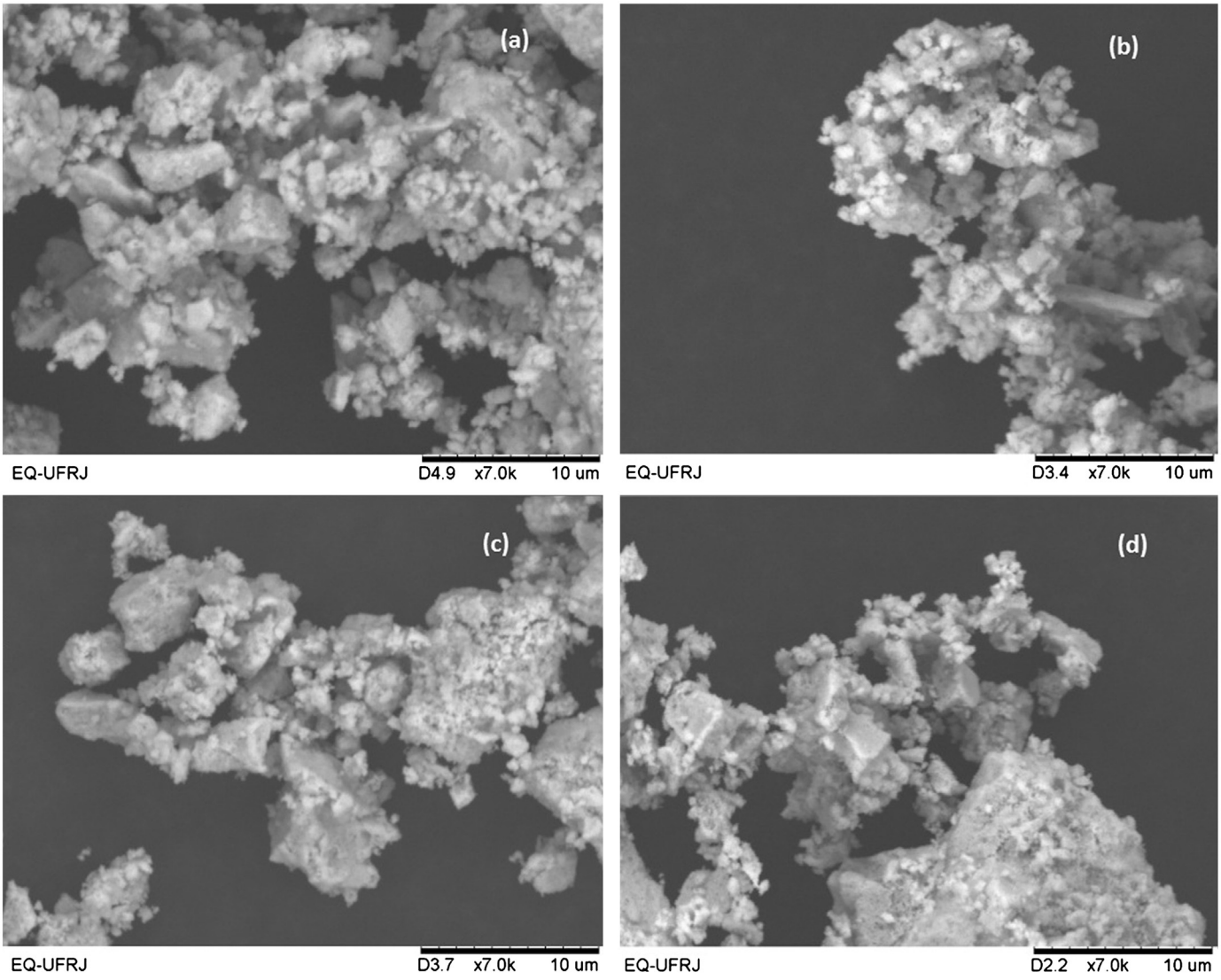

Fig. 3. Micrographs of LSCF powders calcined at different temperatures: (a) 700 °C, (b) 800 °C, (c) 900 °C and (d) 1000 °C.

The milling time used here is much lower than that used in several works of solid state synthesis of LSCF powders. Li et al. [23] and Han et al. [24] milled the oxides/carbonate mixture for 24 h, followed by calcination at 900 and 1000 °C, respectively. Our work pointed out that it is possible to synthesize LSCF powders with single phase using mild conditions: only 4 h of milling and calcination at 800 °C.

3.3. Effect of the sintering temperature

The structure of the LSCF pellets sintered at different temperatures (950–1100 °C) was investigated by XRD, as shown in Fig. 6. All patterns showed pure perovskite phase and no secondary phase was identified. It thus suggests that no phase transition occurred from lower to higher temperatures during the calcination or sintering process of the LSCF powder precursors synthesized by the solid state reaction.

Table 3 shows the average crystallite sizes, microstrain and lattice parameters of the sintered LSCF samples. The crystallite sizes increase with sintering temperature, while there is only a small decrease in microstrain. The rhombohedral structure was maintained in the temperature range investigated, differently from some authors who reported a change of LSCF phase from cubic to rhombohedral when the temperature increases from 800 to 1000 °C [25].

Fig. 7 gives the SEM images of the surface of the sintered pellets. Evidently, with increasing the sintering temperature, the grains agglomerate and grow, and the number of open pores reduces. The sample sintered at 950 °C has a lot of pores of different sizes, while only small pores are observed in the sample sintered at 1100 °C, with a more homogeneous distribution. The porosity of the LSCF pellets measured by Archimedes method is presented in Table 4. The porosity decreases with increasing sintering temperature, as observed in the SEM images. These values are very close to those reported for LSCF samples prepared by the combustion method and sintered in the same temperature range [8]. Li et al. [26] observed a decrease in porosity from 38% to 26% when the

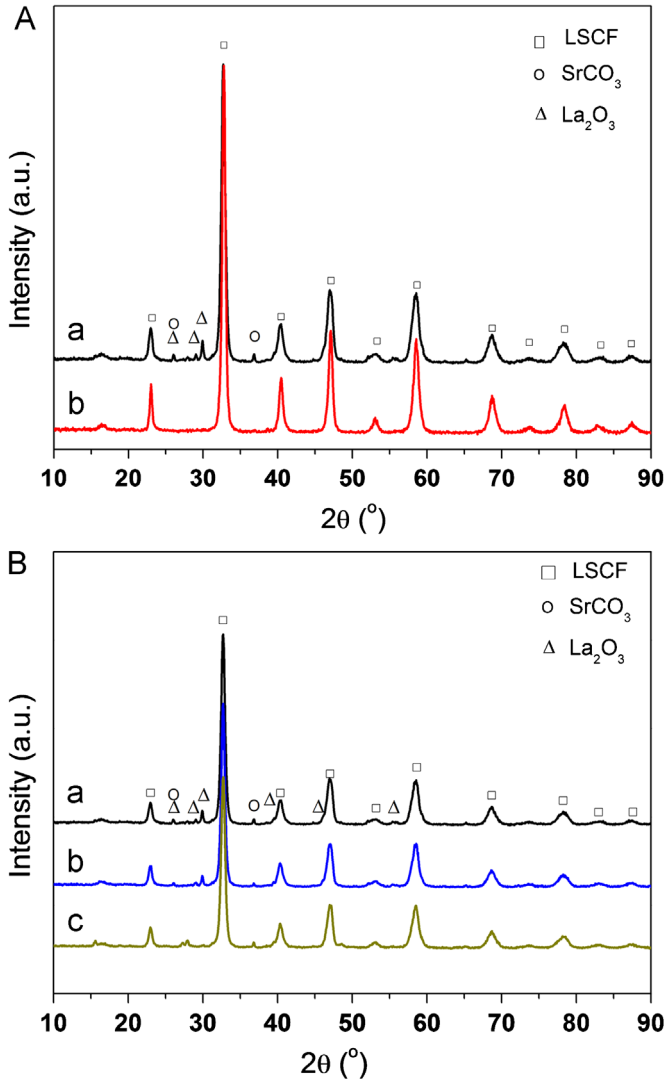

Fig. 4. XRD patterns of the LSCF powders synthesized at 500 rpm, (A) 6 h of milling, with different balls:sample ratios: (a) 6:1 and (b) 8:1, and (B) balls: sample ratio of 6:1, with different milling times: (a) 6 h, (b) 8 h and (c) 10 h.

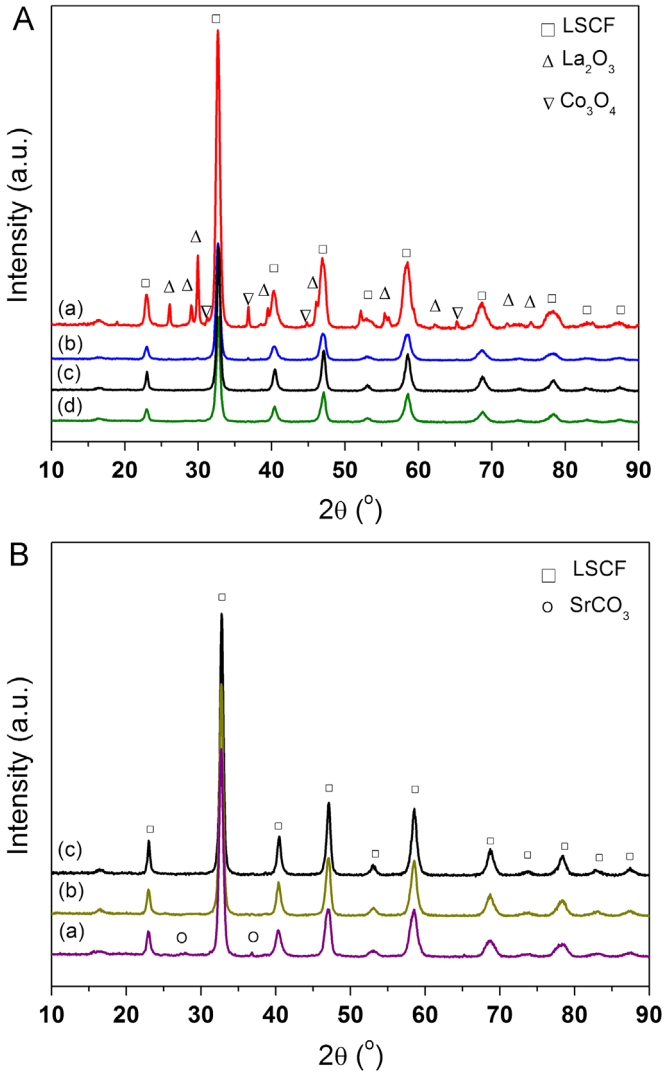

Fig. 5. XRD patterns of the LSCF powders synthesized with balls:sample ratio of 8:1, (A) 6 h of milling and different rotational speeds: (a) 300, (b) 400, (c) 500 and (d) 600 rpm, and (B) 500 rpm and different milling times: (a) 2 h, (b) 4 h and (c) 6 h.

sintering temperature increases from 1000 to 1100 °C, for $La_{0.8}Sr_{0.2}MnO_3$ samples, and they concluded that the proper sintering temperature for cathode application was 1100 °C. The ideal porosity for use as cathode in SOFC is in the range of 20–40% [2].

The perovskite structures doped with transition metal oxides of Fe, Co, Mn, etc. are well known for their mixed ionic and electronic conductivity (MIEC) properties [27,28]. Fig. 8 shows the Arrhenius plots of ln (σT) versus $1/T$ for LSCF pellets sintered at different temperatures. All samples exhibited a linear dependence over a wide range of temperatures (400–1000 °C), as predicated by the following equation:

$$ln(\sigma T) = lnA - \frac{E_a}{RT} \quad (3)$$

where σ, A, T, R and E_a are respectively the conductivity of the material, a constant associated with crystalline structure and composition of material, absolute temperature, gas constant, and activation energy of conductance. The conductivity of the sintered samples increases with temperature, as expected in a semiconducting behavior, which is consistent with small polaron conduction (i.e., localized electronic carriers having a thermally activated mobility) [21,27].

Table 2
Average crystallite size (D_{XRD}), microstrain (ε) and lattice parameters of LSCF powders synthesized with balls:sample ratio of 8:1, 500 rpm and different milling times.

Milling time (h)	D_{XRD} (nm)	ε(%)	Lattice parameters (Å)
2	12.4	0.87	a = 5.4705 ± 0.0050 c = 13.3122 ± 0.0274
4	13.7	0.77	a = 5.4697 ± 0.0046 c = 13.2969 ± 0.0249
6	15.5	0.68	a = 5.4592 ± 0.0032 c = 13.3252 ± 0.0172

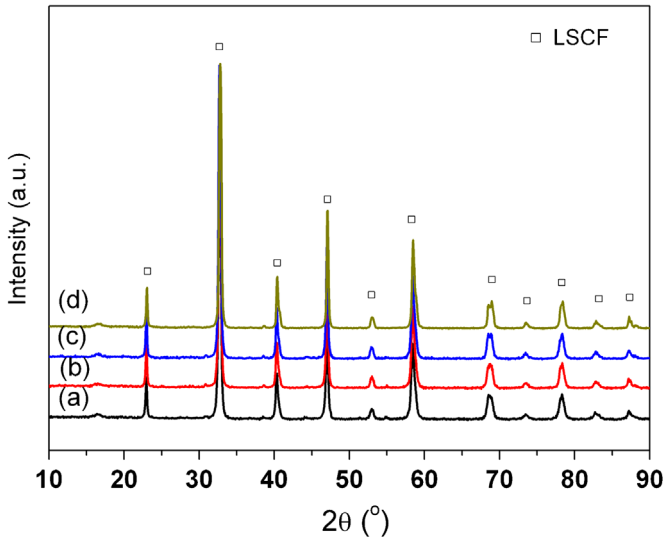

Fig. 6. XRD patterns of LSCF pellets sintered at different temperatures: (a) 950 °C, (b) 1000 °C, (c) 1050 °C, and (d) 1100 °C.

Table 3
Average crystallite size (D_{XRD}), microstrain (ε) and lattice parameters of LSCF samples sintered at different temperatures.

Sintering temperature (°C)	D_{XRD} (nm)	ε(%)	Lattice parameters (Å)
950	25.9	0.40	a = 5.4769 ± 0.0032 c = 13.2929 ± 0.0172
1000	27.3	0.38	a = 5.4743 ± 0.0027 c = 13.3211 ± 0.0145
1050	28.4	0.37	a = 5.4729 ± 0.0022 c = 13.3074 ± 0.0122
1100	31.7	0.31	a = 5.4701 ± 0.0030 c = 13.3093 ± 0.0165

Table 4 shows the conductivity of the samples at 800 °C and the activation energy calculated from the slopes of the Arrhenius curves. The sintering temperature had a negligible effect on the electrical conductivity at high temperatures (> 600 °C), as observed by Kharton et al. [29] for $LaCoO_3$. On the other hand, there is an increase of the activation energy for electrical conduction with the decrease of sintering temperature, which demonstrates the increasing difficulty for the electron conduction with increasing porosity [30].

The values of activation energy reported here are very similar to those of other studies. According to Tai et al. [21], activation energies for $La_{0.8}Sr_{0.2}Co_{1-y}Fe_yO_3$ range from 0.04 to 0.14 eV when y varies from 0 to 1, assuming the adiabatic hopping of small polarons. Dutta et al. [22] calculated the activation energy of conduction in the range of 0.1–1.2 eV for LSCF samples sintered at 900–1100 °C. The activation energy for electrical conduction reported by Pakzad et al. [31] was 0.14 eV for $La_{0.6}Sr_{0.4}Co_{0.2}Fe_{0.8}O_3$ prepared by solid state reaction, calcined at 1000 °C and sintered at 1200 °C.

The conductivity values in this study are much lower than those measured by other authors using the four-probe method. For example, Dutta et al. [22] measured a conductivity of 24 S cm^{-1} at 800 °C for $La_{0.8}Sr_{0.2}Co_{0.8}Fe_{0.2}O_3$ sample sintered at 1050 °C. The value measured by Zeng et al. [30] was 50 S cm^{-1} at 800 °C for $La_{0.6}Sr_{0.4}Co_{0.2}Fe_{0.8}O_3$ sample sintered at 1000 °C. The two-probe method is not appropriate for a precise measurement, and it tends to include a large experimental error in the electric resistance change owing to the electric resistance change at the electrodes. The four point probe is preferable over a two point probe because the contact and spreading resistances associated with the two point probe cannot be measured [32]. The two-probe method was adopted here because of the simplicity; the conductivity values are valuable to indicate a tendency among the samples and calculate the activation energy, not to obtain real values.

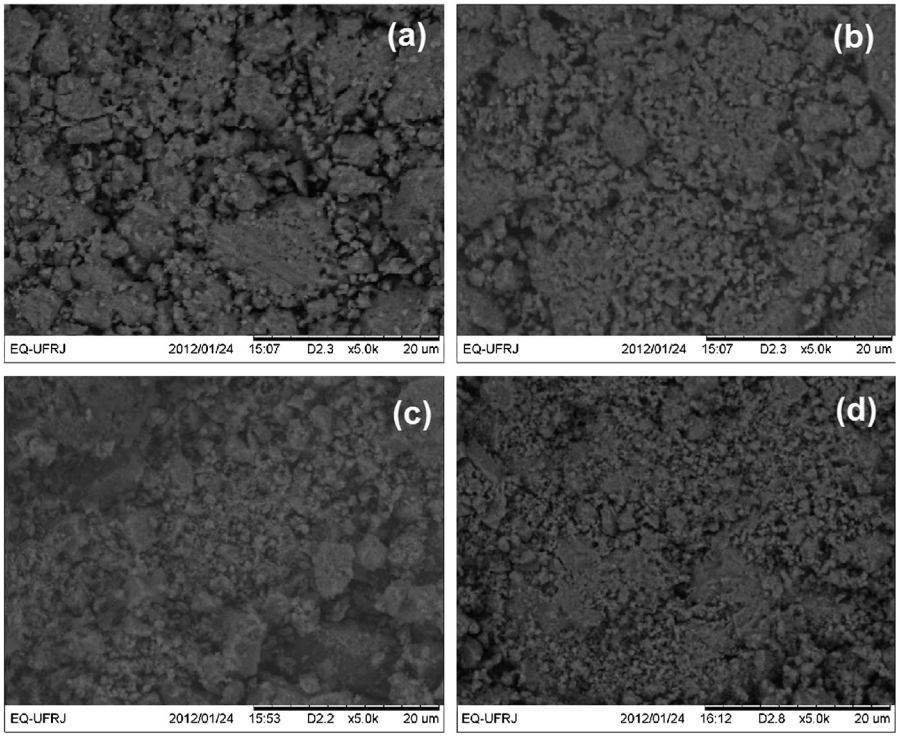

Fig. 7. Micrographs of LSCF pellets sintered at different temperatures: (a) 950 °C, (b) 1000 °C, (c) 1050 °C, and (d) 1100 °C.

Table 4
Porosity, electrical conductivity and activation energy (E_a) of the LSCF pellets sintered at different temperatures.

Sintering temperature (°C)	Porosity (%)	Conductivity at 800 °C (S cm^{-1})	E_a (eV)
950	49.1	0.264	0.154
1000	42.8	0.259	0.111
1050	37.6	0.275	0.109
1100	32.6	0.230	0.070

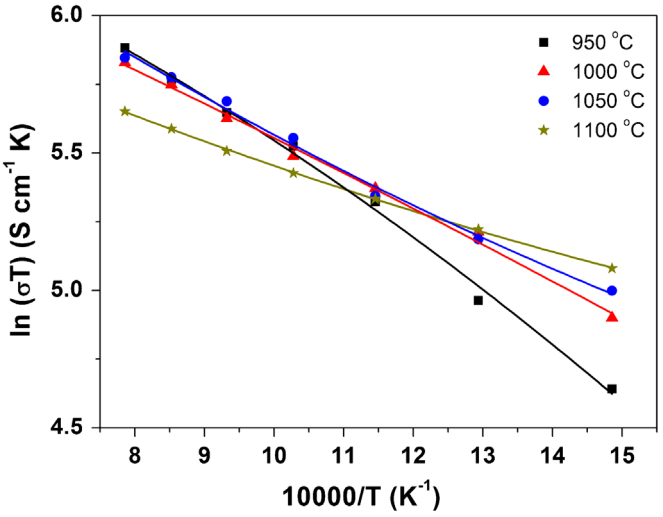

Fig. 8. Electrical conductivity of LSCF pellets as a function of reciprocal absolute temperature, for different sintering temperatures.

4. Conclusions

A solid state reaction from oxides of La, Co, Fe and $SrCO_3$ has been used to prepare LSCF powders using a mechanochemical activation in ball mill, followed by calcination. According to our results, phase formation and crystallite size are strongly dependent on the calcination temperature and milling parameters. The minimum calcination temperature to obtain pure LSCF phase is 800 °C, with complete decomposition of the carbonate precursor. All samples have rhombohedral structure with space group R3c. The crystallite size increases from 9.6 to 26 nm when the calcination temperature increases from 700 to 1000 °C. The powders form loose agglomerates of different sizes. Single LSCF phase formation can be obtained when using balls:sample mass ratio of 8:1, rotational speed of 500 rpm and only 4 h of milling. The porosity of the pellets decreased with increasing sintering temperature, as well as the activation energy for electrical conduction.

Acknowledgments

The authors thank CAPES, FAPERJ and CNPq for financial support granted to carry out this work.

References

[1] M.A. Peña, J.L.G. Fierro, Chemical structures and performance of perovskite oxides, Chemical Review 101 (2001) 1981–2017.
[2] S.C. Singhal, K. Kendall, High Temperature Solid Oxide Fuel Cells: Fundamentals, Design and Applications, Elsevier, 2004.
[3] S.J. Skinner, Recent advances in perovskite-type materials for SOFC cathodes, Fuel Cells Bulletin 33 (2001) 6–12.
[4] A. Mai, V.A.C. Haanappel, S. Uhlenbruck, F. Tietz, D. Stover, Ferrite-based perovskites as cathode materials for anode-supported solid oxide fuel cells. Part I. Variation of composition, Solid State Ionics 176 (2005) 1341–1350.
[5] R.J. Bell, G.J. Millar, J. Drennan, Influence of synthesis route on the catalytic properties of $La_{1-x}Sr_xMnO_3$, Solid State Ionics 131 (2000) 211–220.
[6] M. Gaudon, C. Laberty-Robert, F. Ansart, P. Stevens, A. Rousset, Preparation and characterization of $La_{1-x}Sr_xMnO_{3+\delta}$ ($0 \leq x \leq 0.6$) powder by sol–gel processing, Solid State Sci. 4 (2002) 125–133.
[7] Q. Xu, D. Huang, W. Chen, J. Lee, H. Wang, R.Z. Yuan, Citrate method synthesis, characterization and mixed electronic–ionic conduction properties of $La_{0.6}Sr_{0.4}Co_{0.8}Fe_{0.2}O_3$ perovskite-type complex oxides, Scripta Materialia 50 (2004) 165–170.
[8] L. Conceição, A.M. Silva, N.F.P. Ribeiro, M.M.V.M. Souza, Combustion synthesis of $La_{0.7}Sr_{0.3}Co_{0.5}Fe_{0.5}O_3$ (LSCF) porous materials for application as cathode in IT-SOFC, Materials Research Bulletin 46 (2011) 308–314.
[9] Q. Zhang, F. Saito, Mechanochemical synthesis of $LaMnO_3$ from La_2O_3 and Mn_2O_3 powders, Journal of Alloys and Compounds 297 (2000) 99–103.
[10] L. Conceição, C.R.B. Silva, N.F.P. Ribeiro, M.M.V.M. Souza, Influence of the synthesis method on the porosity, microstructure and electrical properties of $La_{0.7}Sr_{0.3}MnO_3$ cathode materials, Materials Characterization 60 (2009) 1417–1423.
[11] Q. Zhang, T. Nakagawa, F. Saito, Mechanochemical synthesis of $La_{0.7}Sr_{0.3}MnO_3$ by grinding constituent oxides, Journal of Alloys and Compounds 308 (2000) 121–125.
[12] B.D. Stojanovic, Mechanochemical synthesis of ceramic powders with perovskite structure, Journal of Materials Processing Technology 143-144 (2003) 78–81.
[13] Q. Zhang, F. Saito, A review on mechanochemical syntheses of functional materials, Advanced Powder Technology 23 (2012) 523–531.
[14] T. Tsuzuki, P.G. McCormick, Mechanochemical synthesis of nanoparticles, Journal of Materials Science 39 (2004) 5143–5146.
[15] G.K. Williamson, W.H. Hall, X-ray line broadening from filed aluminum and wolfram, Acta Metallurgica 1 (1953) 22–31.
[16] T. Hungria, A. Hungria, A. Castro, Mechanosynthesis and mechanical activation processes to the preparation of the $Sr_2[Sr_{n-1}Ti_nO_{3n+1}]$ Ruddlesden–Popper family, Journal of Solid State Chemistry 177 (2004) 1559–1566.
[17] A. Moure, J. Tartaj, C. Moure, Processing and characterization of Sr doped $BiFeO_3$ multiferroic materials by high energetic milling, Journal of Alloys and Compounds 509 (2011) 7042–7046.
[18] R.V. Wandekar, B.N. Wani, S.R. Bharadwaj, Crystal structure, electrical conductivity, thermal expansion and compatibility studies of Co-substituted lanthanum strontium manganite system, Solid State Science 11 (2009) 240–250.
[19] C. Nityanand, W.B. Nalin, B.S. Rajkumar, C.M. Chandra, Synthesis and physicochemical characterization of nanocrystalline cobalt doped lanthanum strontium ferrite, Solid State Science 13 (2011) 1022–1030.
[20] A. Möbius, D. Henriques, T. Markus, Sintering behaviour of $La_{1-x}Sr_xCo_{0.2}Fe_{0.8}O_{3-\delta}$ ($0.3 \leq x \leq 0.8$) mixed conducting materials, Journal of European Ceramic Society 29 (2009) 2831–2839.
[21] L-W. Tai, M.M. Nasrallah, H.U. Anderson, D.M. Sparlin, S.R. Sehlin, Structure and electrical properties of $La_{1-x}Sr_xCo_{1-y}Fe_yO_3$. Part 1. The system $La_{0.8}Sr_{0.2}Co_{1-y}Fe_yO_3$, Solid State Ionics 76 (1995) 259–271.
[22] A. Dutta, J. Mukhopadhyay, R.N. Basu, Combustion synthesis and characterization of LSCF-based materials as cathode of intermediate temperature solid oxide fuel cells, Journal of European Ceramic Society 29 (2009) 2003–2011.

[23] S. Li, W. Jin, N. Xu, J. Shi, Synthesis and oxygen permeation properties of $La_{0.2}Sr_{0.8}Co_{0.2}Fe_{0.8}O_{3-\delta}$ membranes, Solid State Ionics 124 (1999) 161–170.
[24] D. Han, Y. Okumura, Y. Nose, T. Uda, Synthesis of $La_{1-x}Sr_xSc_{1-y}Fe_yO_{3-\delta}$ (LSSF) and measurement of water content in LSSF, LSCF and LSC hydrated in wet artificial air at 300 °C, Solid State Ionics 181 (2010) 1601–1606.
[25] D. Waller, J.A. Lane, J.A. Kilner, B.C.H. Steele, The effect of thermal treatment on the resistance of LSCF electrodes on gadolinia doped ceria electrolytes, Solid State Ionics 86–88 (1996) 767–772.
[26] G.-J. Li, Z.-R. Sun, H. Zhao, C-H. Chen, R-M. Ren, Effect of temperature on the porosity, microstructure, and properties of porous $La_{0.8}Sr_{0.2}MnO_3$ cathode materials, Ceramics International 33 (2007) 1503–1507.
[27] J.W. Stevenson, T.R. Armstrong, R.D. Carneim, L.R. Pederson, W. J. Weber, Electrochemical properties of mixed conducting perovskites $La_{1-x}M_xCo_{1-y}Fe_yO_{3-\delta}$ (M=Sr, Ba, Ca), Journal of Electrochemical Society 143 (1999) 2722–2729.
[28] A.N. Petrov, V.A. Cherepanov, A.Y. Zuev, Thermodynamics, defect structure, and charge transfer in doped lanthanum cobaltites: an overview, Journal of Solid State Electrochemistry 10 (2006) 517–537.
[29] V.V. Kharton, E.N. Naumovich, A.V. Kovalevsky, A.P. Viskup, F. M. Figueiredo, I.A. Bashmakov, F.M.B. Marques, Mixed electronic and ionic conductivity of $LaCo(M)O_3$ (M=Ga, Cr, Fe or Ni) IV. Effect of preparation method on oxygen transport in $LaCoO_{3-\delta}$, Solid State Ionics 138 (2000) 135–148.
[30] P. Zeng, R. Ran, Z. Chen, H. Gu, Z. Shao, J.C.D. Costa, S. Liu, Significant effects of sintering temperature on the performance of $La_{0.6}Sr_{0.4}Co_{0.2}Fe_{0.8}O_{3-\delta}$ oxygen selective membranes, Journal of Membrane Science 302 (2007) 171–179.
[31] A. Pakzad, H. Salamati, P. Kameli, Z. Talaei, Preparation and investigation of electrical and electrochemical properties of lanthanum-based cathode for solid oxide fuel cell, International Journal of Hydrogen Energy 35 (2010) 9398–9400.
[32] L. Conceição, N.F.P. Ribeiro, M.M.V.M. Souza, Synthesis of $La_{1-x}Sr_xMnO_3$ powders by polymerizable complex method: Evaluation of structural, morphological and electrical properties, Ceramics International 37 (2011) 2229–2236.